Available online at www.sciencedirect.com

ScienceDirect

Energy Procedia 80 (2015) 401 – 410

Energy Procedia

12th Deep Sea Offshore Wind R&D Conference, EERA DeepWind'2015

Passive filter design and offshore wind turbine modelling for system level harmonic studies

Henrik Brantsæter[a,*], Łukasz Kocewiak[b], Atle Rygg Årdal[c], Elisabetta Tedeschi[a]

[a]*Dep. of Electric Power Engineering,Norwegian University of Science and Technology, Trondheim, Norway*
[b]*DONG Energy Wind Power, Fredericia, Denmark*
[c]*SINTEF Energy Research, Trondheim, Norway*

Abstract

This paper is aimed at creating a framework for harmonic studies of an offshore wind power plant by means of system level time domain simulations. Many modern wind turbine generators employ full-scale power electronic converters, thus the filter connected between the power electronic converter and grid becomes a key aspect. The main contribution of the paper is a comparison between eight LCL-filter configurations. The 400 MW Anholt offshore wind power plant off the coast of Denmark, and its 3.6 MW turbines, is considered a reference for this paper.

LCL filters find broad application in the grid integration of power electronic converters. Common practices for the tuning of such filters are therefore examined and adapted to the requirements of a specific test case. Hence, a set of parameters is defined for the LCL filter of a grid connected 3.6 MW wind turbine with a full-scale power electronic converter. LCL filters are further examined through analysis in the frequency domain, focusing on passive damping methods and variations of the capacitive branch which may improve the characteristics of such filters. Finally, a time-domain model of a grid-connected wind turbine inverter is established. Eight different LCL-filter configurations are implemented and compared in terms of harmonic content and losses. It is shown how dedicated additional branches are able to reduce both losses and harmonic content. This analysis is carried out using open-loop converter control system. A simple model including the full control system is constructed and outlined in a separate section.

Peer-review under responsibility of SINTEF Energi AS

Keywords: offshore wind power; wind energy; passive filter design; LCL filter; harmonics

1. Introduction

The number of offshore wind power plants (WPPs) is rapidly increasing around the world, and especially in European countries like the UK, Germany and Denmark. Modern variable speed turbines use advanced power electronic converters in the MW range [1]. Many of the wind turbine manufacturers are these days offering their flagship products with fully-rated back-to-back converters [2]. Wind turbine generators (WTGs) installed offshore are connected together by widespread networks of sub-marine power cables. These offshore networks are connected to on-shore

* Corresponding author. Tel.: +47-951-11-461
E-mail address: brantsat@stud.ntnu.no

Peer-review under responsibility of SINTEF Energi AS
doi:10.1016/j.egypro.2015.11.444

transmission systems by medium or high voltage sub-marine cables. Such grid connections has lead to challenges for the industry in terms of grid operation, harmonic emissions, stability and control [3]. The rapid development of wind power is nowadays also reflected in grid codes, which require WPPs to operate much like conventional power plants, e.g. contribute to frequency and voltage support. Grid codes also regulate behaviour during abnormal operating conditions like network faults and require WPPs to help maintain acceptable power quality by adhering to strict limits on harmonic distortion [1,4].

In case of small distributed wind generation, performing sophisticated harmonic studies has not been the norm, as such generation has rather limited impact on larger power systems. Simplified assessment methods have usually been adopted, providing fast results based on conservative assumptions [5]. However, for large WPPs with capacity in the range of several hundred MW, analysis of harmonics becomes an important part of the system planning [6].

2. Harmonic emissions and filtering

The proliferation of power electronics in power systems has caused national and international agencies to develop standards and regulations regarding harmonics. IEEE Std. 519-2014 contains recommended limits on harmonic currents injected by non-linear loads as well as the quality of voltage a utility should be able to supply to a consumer at any point in a distribution system. A utility should be able to supply voltage of the quality given in the standard as long as the harmonic currents injected by generators and consumers are limited according to the values given in the standard [7]. The suggested limits on harmonic currents can be used as guidance for filter design when grid characteristics are unknown [8].

When selecting a filter for a WTG with a full-scale converter, parameters like efficiency, weight, volume and cost must be considered. Weight and volume are critical in WTGs, and especially for offshore applications. The cost of a filter depends mostly on the amount of material used. For the grid connection of a converter in the MW range, a pure inductive filter requires a value of inductance which is too large, and therefore has unacceptable voltage drop across it. A large inductor also causes poor controller bandwidth. LCL filters have low dependency on grid parameters, which is of major importance in high power applications. They also provide better attenuation than other filters of similar size, and they have inductive outputs, which is important to limit current inrush problems [8].

2.1. Selction of LCL filter parameters

Tuning of LCL filters has been discussed extensively in literature [8–12]. Specific constraints on each element of the filter varies to some degree with filter application, power-level and sensor placement for the controllers; however, the main principles typically used for the design of LCL filters remain the same. Those principles are outlined in this section. In order to comply with standards and grid codes, most authors suggest the peak to peak ripple of the output current should be limited to less than 2 % of the rated fundamental current amplitude.

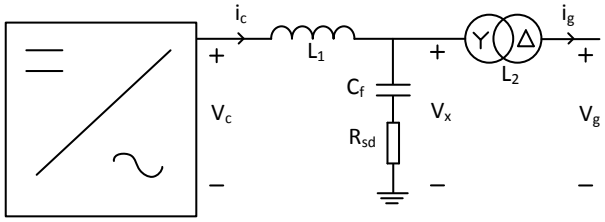

Fig. 1. LCL filter with components nomenclature

First, the base parameters using a conventional per unit system are calculated. The rated power of the converter, S_n, is selected as the power base, and the RMS line-to-line voltage, $V_{LL,rms}$, is selected as the voltage base.

$$S_{base} = S_n; \quad V_{base} = V_{LL,rms}; \quad Z_{base} = \frac{V_{base}^2}{S_{base}}; \quad L_{base} = \frac{Z_{base}}{\omega_n}; \quad C_{base} = \frac{1}{\omega_n Z_{base}}; \quad I_{base} = \frac{S_{base}}{\sqrt{3}V_{base}}; \quad \omega_n = 2\pi f_n$$

The value of inductor L_1 is usually selected independently, and by itself it should able to limit the ripple of the converter output current to 10 % of the rated current amplitude. Equation 1 estimates the necessary value of inductance

given a DC side voltage of V_{dc}, a duty cycle D, maximum peak-to-peak current ripple $\Delta i_{imax,p\text{-}p}$, and PWM switching frequency f_{sw} of the converter. Maximum ripple occurs for duty cycle D=0.5, and the inductor is therefore selected using this value. The equation is only valid for a two-level converter. If a three-level converter is used, the expression can be divided by a factor of two in order to obtain the necessary inductance.

$$L_1 = \frac{(V_{dc} - DV_{dc})D}{2\Delta i_{imax,p-p} f_{sw}} = \frac{V_{dc}}{8\Delta i_{imax,p-p} f_{sw}} \qquad where, \qquad \Delta i_{imax,p-p} = 0.1\sqrt{2} I_{base} \tag{1}$$

The capacitor is typically selected to provide reactive power of about 5 % of the rated power of the converter, as given by equation 2. A larger capacitor is sometimes suggested for specific applications. For the same current output ripple, a larger value of capacitance allows for using a smaller value of inductance for L_1, but also lead to a higher current drawn from the converter and thus reduces efficiency.

$$C_f = 0.05 C_{base} = 20\,\text{pu} \tag{2}$$

Equation 3 relates the harmonic current supplied by the converter to the harmonic current which is injected to the grid. By solving equation 3 for x with a given attenuation factor k_a, the necessary value of L_2 can be determined. If k_a is set to 20 %, the total attenuation, found by multiplying the two attenuation factors of 20 % and 10 %, equals the target value of 2 % ripple. As indicated in Fig. 1, the WTG transformer inductance should be considered part of L_2.

$$\frac{i_g(h)}{i_c(h_{sw})} = k_a = \frac{1}{|1 + x[1 - L_1 C_f \omega_{sw}^2]|} \qquad where, \qquad x = \frac{L_2}{L_1} \tag{3}$$

Unlike a simple L filter, an LCL filter has a resonance which must be taken into consideration. The resonance frequency of the filter is given by equation 4. In order to avoid resonance problems in the lower and upper parts of the harmonic spectrum, it should be verified that the filter parameters comply with the constraint of equation 5.

$$f_{res} = \frac{1}{2\pi}\sqrt{\frac{L_1 + L_2}{L_1 L_2 C_f}} \tag{4}$$

$$10 f_1 \leq f_{res} \leq 0.5 f_{sw} \tag{5}$$

To suppress oscillations around the resonance frequency, some sort of damping must be inserted. The simplest form of damping involves inserting a resistor in the capacitive branch with a value equal to one third of the capacitive reactance at the resonance frequency.

$$R_{sd} = \frac{1}{3\omega_{res} C_f} \tag{6}$$

However, the damping resistor will cause fundamental frequency losses and negatively affects the filter performance.

2.2. Filter design calculation example

The WTG which is used as a test case in this section is assumed to be similar to the 3.6 MW Siemens SWT-3.6-120. This turbine is used in several offshore WPPs, including the 400 MW Anholt WPP in Denmark [13]. The converter is estimated to have a rated power of 5 MVA, a DC side voltage of 1.2 kV, rated line-to-line AC side voltage of 690 V, and a PWM switching frequency of 2.5 kHz. The resulting per unit bases are shown in table 1. Parameters for a 5 MVA transformer have been estimated from available data on a specific type of transformer for wind turbine applications [14]. The complete set of parameters for the transformer is listed in Table 4, but for filter design only the total series inductance of 7.5 % is used.

Table 1. Per unit system bases used for filter design

Per unit bases	
S_b	5 MVA
V_b	690 V
Z_b	95.22 mΩ
L_b	303.1 µH
C_b	33.43 mF
I_b	4.184 kA

Table 2. Calculated LCL filter parameters using standard procedure

Parameter	Per unit value	LV side abs. value
Converter side inductance L_1	0.3346	101.4 µH
Filter capacitor C_f	20.0	1.671 mF
Grid side inductance L_2	0.0492	14.91 µH
Damping resistor R_{sd}	0.3087	29.39 mΩ

LCL filter parameter values resulting from the procedure explained in section 2.1 are given in table 2. They correspond to a resonant frequency of 1080 Hz, which is within the required range of equation 5. However, to obtain an acceptable voltage drop and controller bandwidth, the converter side inductance should be limited to 0.10 pu. Also, the calculated value of the grid side inductor L_2 is less than the total series inductance of the transformer. Enforcing these additional constraints on maximum value of L_1 and minimum value of L_2 results in a new set of parameters. By examining the equations used in the design procedure explained above, it however becomes apparent that the filter performance with these parameters is reduced, and a ripple current of 2 % will not be achieved. The converter side inductance L_1 only attenuates the current ripple to 33.4 % of the rated current in accordance equations 1. The corresponding value of k_a has decreased to 13.1 %. Overall it results in an estimated output current ripple of 4.34 %.

There are several ways in which the objective of 2 % ripple can be achieved with the additional restrictions on the size of the inductors. Equation 1 shows that an increase in the switching frequency will decrease the necessary size of L_1. This may however be undesirable, because it also increases switching losses and cooling requirements. Another option is to use a different converter topology which produces a lower ripple, for example a three-level neutral point clamped topology. The most convenient solution in this case, however, seems to be an increase in the capacitive reactance by reducing C_f to 10.15 pu. The attenuation factor k_a is then reduced to 6.0 %, and the overall objective of 2 % current ripple is achieved. Otherwise a trade-off must be made between voltage drop, controller bandwidth, and current ripple.

For this example, a decrease in capacitor value to 10.15 pu is suggested in order to achieve the attenuation objective. In other words the shunt branch will supply approximately 0.5 MVAr in steady state. This is largely compensated for by the inductive reactance of the filter, and the converter provides flexibility to control reactive power supplied to the grid. The suggested solution parameters for the LCL filter of the example are therefore as given in table 3. The filter resonance with these parameters appears at 769.5 Hz.

Table 3. Suggested solution of LCL filter design calculation example

Parameter	Per unit value	LV side abs value
Converter side inductance L_1	0.10	30.31 µH
Filter capacitor C_f	10.15	3.293 mF
Grid side inductance L_2	0.075	22.73 µH
Damping resistor R_{sd}	0.2198	20.93 mΩ

2.3. Frequency domain analysis of filters

The LCL filter values of table 3 will be used as a basis for analysing filter performance by means of bode plots. The values of L_1 and L_2 are considered fixed, and the suggested values of C_f and R_{sd} are used unless other values are clearly specified. Parasitic resistance of inductors and capacitor is neglected.

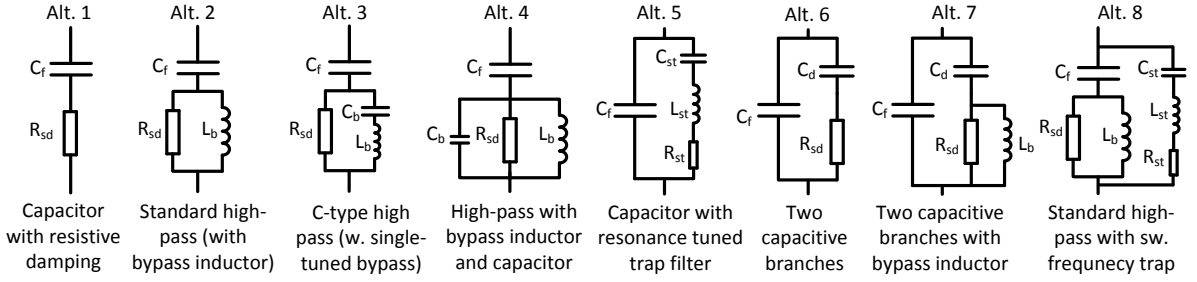

Fig. 2. Shunt branch topologies for LCL filter with components nomenclature

The capacitor of an LCL filter is essentially a high-pass filter, providing a low impedance path to ground for high frequency components of the current. Fig. 2 shows some of the many possible variants which can constitute the shunt branch of the an LCL filter. The use of additional elements compared to a simple shunt capacitor is aimed at improving one or more of the following performance indicators:

- Overall attenuation of harmonics
- Damping of the LCL filter resonance

- Power losses caused by the damping resistor

By plotting transfer functions of LCL filters with different variants of the shunt branch, attenuation of harmonic components and damping of the filter resonance can be compared. Of particular interest is the transfer function relating the applied voltage from the converter side and the resulting current at the outgoing terminals of the filter. This will be referred to as the filter trans-admittance, and is defined by equation 7. The grid side self-admittance is the admittance seen from open grid side terminals of the filter, as defined by equation 8. It can be used to investigate parallel resonances seen from the grid side.

$$Y_{cg}(s) = \frac{i_g(s)}{v_c(s)} \tag{7}$$

$$Y_{gg}(s) = \frac{i_g(s)}{v_g(g)} \tag{8}$$

For a pure inductive filter, the trans-admittance is simply given by equation 9. For an LCL filter with a resistor installed in series with the capacitor, the trans-admittance is given by equation 10. The trans-admittance of an undamped LCL filter can be found by setting R_{sd} equal to zero.

$$Y_{cg,L}(s) = \frac{1}{s(L_1 + L_2)} \tag{9}$$

$$Y_{cg,LCL}(s) = \frac{C_f R_{sd} s + 1}{L_1 L_2 C_f s^3 + C_f (L_1 + L_2) R_{sd} s^2 + (L_1 + L_2) s} \tag{10}$$

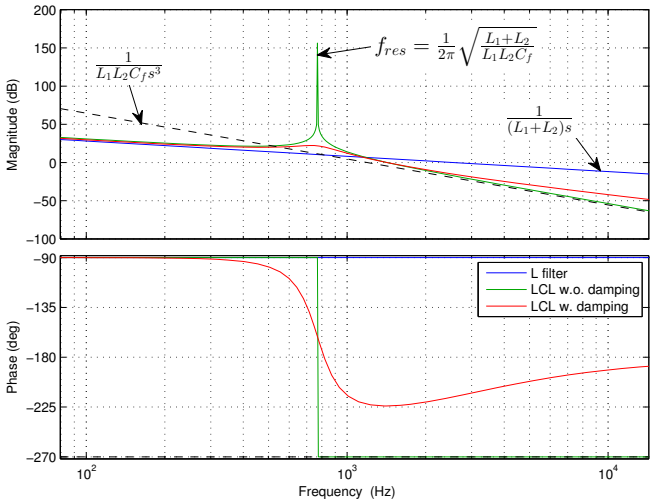

Fig. 3. Characteristic transfer function responses of L filter, undamped LCL filter and damped LCL filter (Alt. 1)

Fig. 3 shows the trans-admittance of an L filter, an undamped and a damped LCL filter (Alt. 1). The L filter has simply been constructed by removing the capacitive shunt branch, keeping the inductance values constant. The LCL filter resonance is well damped when installing a resistor in accordance with equation 6. From equation 10 one can see that the introduction of resistor R_d reduces the roll off of the trans-admittance from 60 dB to 40 dB. The roll of indicates attenuation performance of high frequency harmonics, most importantly the sideband harmonics around multiples of the switching frequency. Hence the 60 dB per decade asymptote of the undamped filter is plotted in all bode diagrams for easy comparison of roll off.

As explained in section 2.1 and illustrated in Fig. 3, inserting a resistor in series with the capacitor of the LCL filter provides damping of the filter resonance at the expense of increased losses and reduced attenuation of high-order harmonics. The standard high-pass filter and C-type filter, illustrated respectively as Alt. 2 and Alt. 3 in Fig. 2, allow for reducing losses while still providing damping of the filter resonance. The standard high-pass filter achieves this by having an inductor in parallel with the damping resistor. This inductor reduces losses by providing an alternative path for the current at fundamental frequency. Alzola et al. [15] suggest choosing equal impedance ratios of the resistor and inductor at fundamental frequency and resonance frequency, as given by equation 11. For the considered test case, this results is an inductor value of 16.99 µH.

$$\frac{R_{sd}}{L_b\omega_1} = \frac{L_b\omega_{res}}{R_{sd}} \quad \longrightarrow \quad L_b = \frac{R_{sd}}{\sqrt{\omega_1\omega_{res}}} \tag{11}$$

The C-type high-pass filter (Alt. 3) has an LC branch which is tuned to the fundamental frequency in parallel with the resistor, thus bypassing the resistor and minimising losses at fundamental frequency. The alternative paths at fundamental frequency provided by the standard and C-type high pass filter topologies have little impact on damping of the filter resonance and high-frequency attenuation. The transfer function responses of the standard high-pass filter (Alt. 2) and C-type high pass filter (Alt. 3) are therefore similar to the one of the simple RC branch (Alt. 1), as illustrated in Fig. 3.

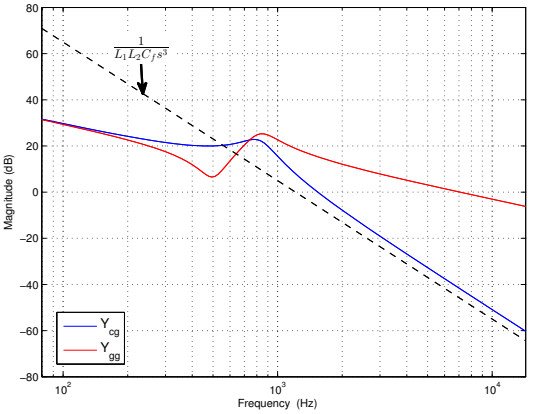

Fig. 4. Transfer function responses of high-pass filter with bypass inductor and capacitor (Alt. 4)

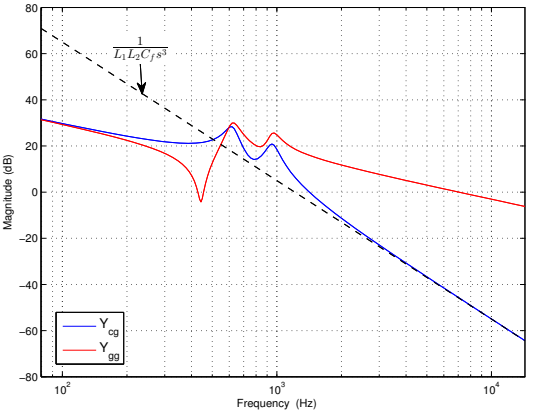

Fig. 5. Transfer function responses of high-pass filter with resonance-tuned trap filter (Alt. 5)

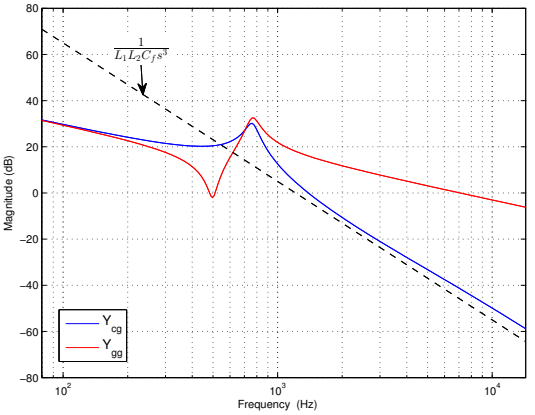

Fig. 6. Transfer functions responses with two capacitive branches and no bypass (Alt. 6)

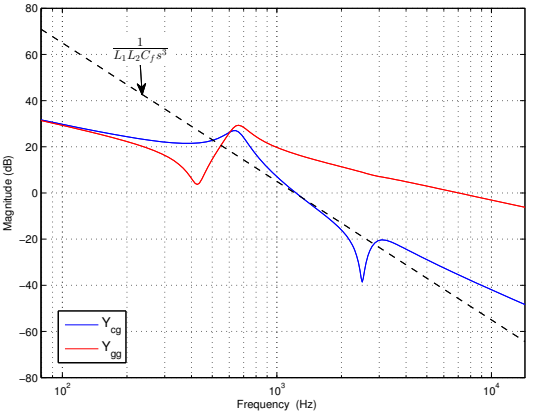

Fig. 7. Transfer function responses with standard high-pass and sw. freq. trap filter (Alt. 8)

The standard high-pass filter can be expanded further by adding a bypass capacitor C_b in parallel with the resistor R_{sd} and inductor L_b, in which case the capacitor is designed to be the dominant current path at high frequency. Alzola et al. [15] suggest choosing equal impedance ratios of the resistor and capacitor at the resonance frequency and at the switching frequency, as given by equation 12. For the considered test-case, this results in a value of 5.482 mF for the bypass capacitor. Fig. 4 shows the transfer function responses of a filter with both bypass inductor and bypass capacitor (Alt. 4); the bypass capacitor contributes to improved attenuation at high frequencies.

$$\frac{R_{sd}}{(\frac{1}{C_b\omega_{res}})} = \frac{(\frac{1}{C_b\omega_{sw}})}{R_{sd}} \quad \longrightarrow \quad C_b = \frac{1}{R_{sd}\sqrt{\omega_{res}\omega_{sw}}} \tag{12}$$

An alternative to resistive damping of the LCL filter resonance involves having a single tuned filter which is tuned to the resonance frequency in parallel with the capacitor (Alt. 5). In theory this kind of filter has very good performance;

it dampens the resonance without reducing attenuation in the upper range of frequencies. In practice, however, the resonance frequency may to some extent change with varying grid impedance. Because the single tuned harmonic filter has a narrow bandwidth, the damping performance may become poor if the actual resonance moves away from the tuned frequency [10].

Fig. 5 shows the transfer function responses with damping provided by a single tuned filter. Capacitance C_{st} of the single tuned filter branch has been set to $0.02C_b$ or 50 pu, while C_f in the primary capacitive branch remains unchanged. The parameters of the single tuned branch in terms of nominal reactive power, tuned frequency and quality factor are equal to 2 % (or 100 kVAr), 769.5 Hz and 3.695 respectively for the plotted curves.

Another approach to reduce the negative impact on high frequency attenuation caused by resistive damping is to split the capacitive branch into two branches (Alt. 6 and Alt. 7). Inserting a resistor in only one of these branches will dampen the resonance. Larger capacitance ratio C_d/C_f and larger resistor R_{sd} provides better damping, but reduces high frequency attenuation. It has been suggested that the best performance is achieved when the capacitance is split equally between the two branches [16]. Moreover, two branches carrying half of the fundamental frequency current each will lead to a reduction of power losses, although a larger resistor may be necessary to provide sufficient damping. By inserting an inductor in parallel with the resistor, losses at the fundamental frequency can be reduced further (Alt. 7). Such an inductor can be tuned using equation 11. When tuned this way, the transfer functions responses for the two alternatives with and without a bypass inductor are near indistinguishable. Fig. 6 shows the transfer function responses of an LCL filter with two capacitive branches (Alt. 6). For the plotted curves, the capacitance of the suggested design is split equally between the two branches, and the damping resistor has a value of 0.330 pu.

For a two-level pulse-width modulated converter, the characteristic current harmonics which exist as side-bands around multiples of the switching frequency are likely to be the most prominent. To specifically suppress these harmonics, one option is to install an additional single tuned trap filter in parallel with a standard high-pass filter. When several passive filters are installed in parallel, there is potential for them to create new resonances, and it is therefore relevant to see how an additional single tuned filter affects the transfer function responses of Y_{cg} and Y_{gg}.

Fig. 7 shows the transfer function of an LCL filter with a standard high-pass and a single tuned filter installed in parallel, as illustrated by Alt. 8 of Fig. 2. The parameters of the single tuned filter in terms of nominal reactive power, tuned frequency and quality factor are respectively equal to 3.0 % (or 150 kVAr), 2500 Hz and 30. From the figure, one can see that no new resonances are introduced in the self-admittance, while the trans-admittance has much better attenuation around the switching frequency. The trap filter has a negative impact on attenuation level at higher frequencies.

2.4. Analysis of filters by means of open loop time-domain simulation

A simple circuit for comparing filter performance has been set up in MATLAB Simulink with SimPowerSystems. The test circuit includes a two-level grid side converter which is controlled in open loop, the filter to be tested, and a stiff voltage source at the grid side terminal of the filter. Assuming there are no interfering resonances upstream of the voltage source, and because all source impedance has been neglected, the results provided with this set-up is considered to indicate the worst case solution. The converter side filter inductor L_1 is modelled with a reactance of 0.10 pu and a resistance of 0.01 pu. The WTG transformer is modelled with a pre-built block from the SimPowerSystems library and the parameters of table 4. The 5 MVA converter is tuned to provide approximately the rated WTG active power of 3.6 MW at unity power factor.

Table 4. WTG transformer data

5 MVA Δ-Y WTG transformer	
Rated voltage	33 kV/690 V
Primary side inductance	0.0375 pu
Primary side resistance	2.675×10^{-3} pu
Secondary side inductance	0.0375 pu
Secondary side resistance	2.675×10^{-3} pu
Shunt inductance	50 pu
Shunt resistance	870 pu

Fig. 8 exemplifies the waveforms and corresponding harmonic frequency spectra of both the converter side and grid side currents for an LCL filter. From the figure it is clear that the 48th and 99th harmonics constitute the largest of the

sideband harmonics in the first and second carrier groups respectively. Consequently, knowledge of the magnitude of these components gives close to full overview of the harmonics.

Fig. 9 shows a comparison of the 48th and 99th harmonics for the eight different LCL filter alternatives. In order to comply with the current distortion limits of IEEE Std. 519-2014, the harmonic current components above the 35th order should be limited to less than 0.3 % of the fundamental. Only the grid current produced with filter alternative 8 has a 48th harmonic component below this limit.

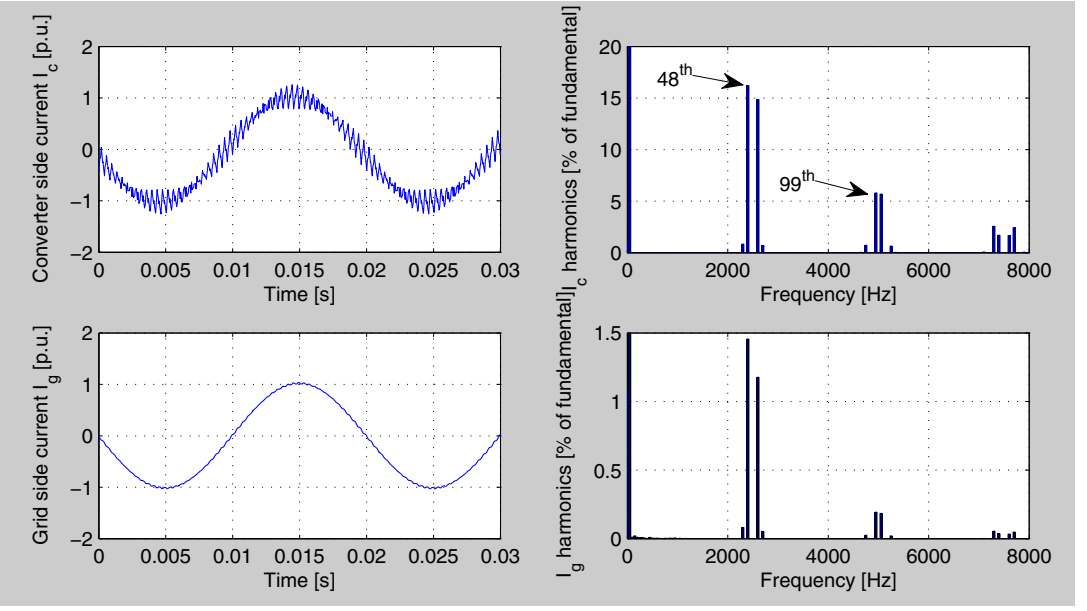

Fig. 8. Example of current waveforms and corresponding frequency spectrums

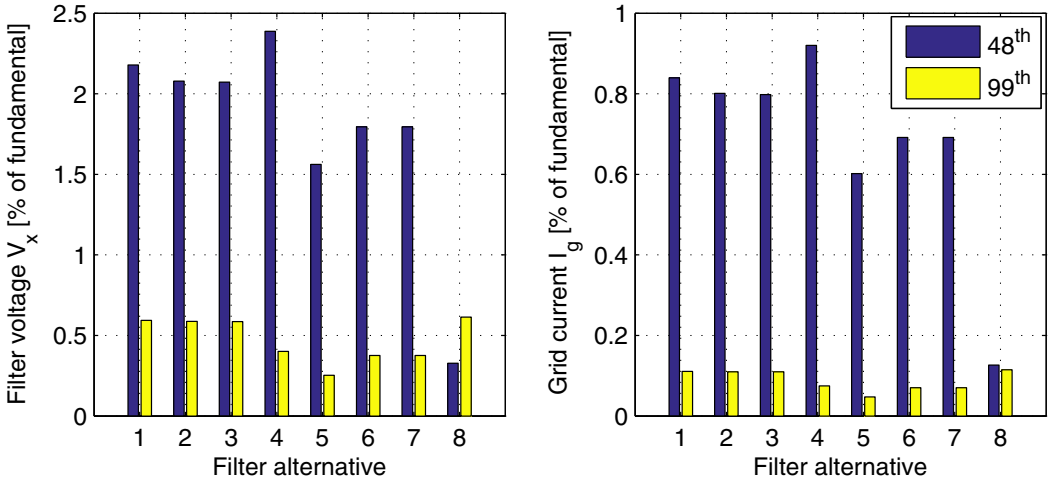

Fig. 9. Comparison of 48th and 99th harmonic for filter alternatives

Table 5. Simulation results & filter data

Topology/Alt. #	1	2	3	4	5	6	7	8
THD_i of output current [%]	1.10	1.05	1.05	1.17	0.77	0.91	0.89	0.26
Fundamental frequency losses [W]	10 750	660	≈ 0	675	1783	4034	248	766
Inductance of shunt branch [μH]	-	16.99	16.99	16.99	80.98	-	25.48	21.02
Capacitance of shunt branch [mF]	3.294	3.294	599.8	8.775	3.962	3.294	3.294	4.297

Table 5 displays simulation results in terms of THD_I and fundamental frequency losses for the different filter topologies defined in Fig. 2. It also shows the total inductance and capacitance of the shunt branch for the compared topologies, which are indicators of cost. Alternative 1 with a simple RC shunt branch, which does not have any bypass of the damping resistor at fundamental frequency, has the largest fundamental frequency losses. The additional components necessary for the more advanced topologies increases the complexity and possibly also the cost of these designs.

3. Control of voltage source converters

An integrated simulation model of an offshore WPP for harmonic studies should include the converter controllers because they may interact with harmonics in the offshore power grid. A simulation model of a voltage source converter (VSC) with vector control in the synchronous reference frame has therefore been implemented.

Control of VSCs in the synchronous reference frame has been discussed extensively in literature [17,18]. PI regulators are typically used in a cascaded control structure, where the fast dynamics of the inner current loops make it possible for the outer voltage loops to provide the reference values for the inner loops. The dq reference frame is selected in such a way that the d-axis is aligned with the voltage phasor of phase a. The instantaneous angle of the rotating d-axis with respect to the fixed a-axis is calculated using a phase locked loop (PLL). Feed-forward terms in the control are used to eliminate the cross coupling. The regulator is tuned using the Modulus Optimum Criterion.

The constructed simulation model is based on the assumption that the back-to-back connected converters of a WTG with fully rated power electronics can be considered decoupled, hence only the grid side VSC is modelled. Only the inner current loops and their regulators have been implemented, hence neglecting any impact of the outer loops. A constant DC side voltage is assumed. The implemented control is shown in Fig. 10.

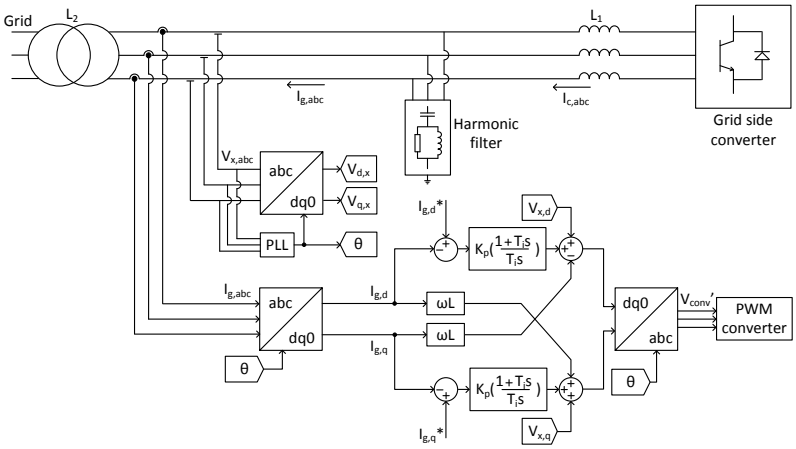

Fig. 10. Implementation of converter dq-axis current control loops

4. Conclusions

This paper aims to constitute a starting point for the construction of an integrated simulation model which captures all of the relevant aspect for investigating harmonics in offshore wind farms. In this regard, the topology and tuning of wind turbine filters has been discussed and analysed. Modeling techniques in both time- and frequency domains are presented, both regarding passive component and the wind turbine converter with its control system.

There are challenges and trade-offs in the tuning process of LCL filters which have been emphasised in this paper. It was shown how filter performance can be analysed by using transfer functions. LCL filters with eight different configurations of the shunt branch were analysed and compared in both frequency domain and time domain. It was shown how the filter topologies providing the best results, at the expense of added complexity, specifically address issues like fundamental frequency losses and attenuation of higher order harmonics.

The fundamental components of the LCL filter, e.g. the converter side inductor, grid side inductor and shunt capacitor, were in the outlined tuning procedure selected to achieve a certain ripple factor which normally is considered sufficient to comply with relevant grid codes. Yet, comparing the frequency spectra of the investigated alternative topologies, an additional branch tuned to the switching frequency seems necessary to guarantee grid code compliance. It is therefore the only solution which can be recommend. However, other considerations such as controller robustness and effect of source inductance may give rise to a different conclusion, hence further investigation is recommended.

References

[1] Blaabjerg, F., Ma, K.. Future on power electronics for wind turbine systems. Emerging and Selected Topics in Power Electronics, IEEE Journal of 2013;1(3):139–152.

[2] Kocewiak, Ł.H., Hjerrild, J., Bak, C.L.. Harmonic analysis of offshore wind farms with full converter wind turbines. In: 8th International Conference on Large-Scale Integration of Wind Power into Power Systems. 2009, p. 1–6.

[3] Kocewiak, Ł., Hjerrild, J., Bak, C.. Wind turbine converter control interaction with complex wind farm systems. Renewable Power Generation, IET 2013;7(4):380–389.

[4] Tsili, M., Papathanassiou, S.. A review of grid code technical requirements for wind farms. Renewable Power Generation, IET 2009;3(3):308–332.

[5] Papathanassiou, S., Papadopoulos, M.. Harmonic analysis in a power system with wind generation. Power Delivery, IEEE Transactions on 2006;21(4):2006–2016.

[6] Kocewiak, Ł.H., Bak, C.L., Hjerrild, J.. Harmonic aspects of offshore wind farms. In: The Danish PhD Seminar on Detailed Modelling and Validation of Electrical Componentes and Systems 2010. 2010, p. 40–45.

[7] Mohan, N., Undeland, T.M., Robbins, W.P.. Power electronics, Converters, Applications and Design. John Wiley & Sons; 2003.

[8] Araujo, S., Engler, A., Sahan, B., Antunes, F.. LCL filter design for grid-connected NPC inverters in offshore wind turbines. In: Power Electronics, 2007. ICPE '07. 7th Internatonal Conference on. 2007, p. 1133–1138.

[9] Reznik, A., Simoes, M., Al-Durra, A., Muyeen, S.. LCL filter design and performance analysis for grid-interconnected systems. Industry Applications, IEEE Transactions on 2014;50(2):1225–1232.

[10] Wang, T.C., Ye, Z., Sinha, G., Yuan, X.. Output filter design for a grid-interconnected three-phase inverter. In: Proc. of IEEE 34th Annual Power Electronics Specialist Conference (PESC 03). 2003, p. 779–784.

[11] Leon, A., Solsona, J.. Performance improvement of full-converter wind turbines under distorted conditions. Sustainable Energy, IEEE Transactions on 2013;4(3):652–660.

[12] Beres, R., Wang, X., Blaabjerg, F., Bak, C., Liserre, M.. A review of passive filters for grid-connected voltage source converters. In: Applied Power Electronics Conference and Exposition (APEC), 2014 Twenty-Ninth Annual IEEE. 2014, p. 2208–2215.

[13] Kocewiak, Ł.H., Øhlenschlæger Kramer, B.L., Holmstrøm, O., Jensen, K.H., Shuai, L.. Active filtering application in large offshore wind farms. In: Integration of Wind Power into Power Systems as well as Transmission Networks for Offshore Wind Farms, Energynautics GmbH, 11-13 November 2014, Berlin, Germany. 2014, p. 1–6.

[14] Technical data EcoDry dry-type transformers. ABB; 2013.

[15] Pena-Alzola, R., Liserre, M., Blaabjerg, F., Sebastián, R., Dannehl, J., Fuchs, F.W.. Analysis of the passive damping losses in LCL-filter-based grid converters. Power Electronics, IEEE Transactions on 2013;28(6):2642–2646.

[16] Channegowda, P., John, V.. Filter optimization for grid interactive voltage source inverters. Industrial Electronics, IEEE Transactions on 2010;57(12):4106–4114.

[17] Haileselassie, T.M., Molinas, M., Undeland, T., et al. Multi-terminal vsc-hvdc system for integration of offshore wind farms and green electrification of platforms in the north sea. In: Nordic Workshop on Power and Industrial Electronics (NORPIE/2008), June 9-11, 2008, Espoo, Finland. Helsinki University of Technology; 2008, p. 1–8.

[18] Bajracharya, C., Molinas, M., Suul, J.A., Undeland, T.M., et al. Understanding of tuning techniques of converter controllers for vsc-hvdc. In: Nordic Workshop on Power and Industrial Electronics (NORPIE/2008), June 9-11, 2008, Espoo, Finland. Helsinki University of Technology; 2008, p. 1–8.